



Assessment of C-band SAR Interferometric Products for Land Cover Classification

Shelton Padua¹, Vinay Kumar Sehgal² and Kishan Singh Rawat²

¹ICAR – National Bureau of Soil Survey and Land Use Planning, Regional Centre, Jorhat-785004, India

²Division of Agricultural Physics, Indian Agricultural Research Institute, New Delhi – 110012, India

Abstract: Up to date information regarding the land cover types are required for environmental monitoring and remote sensing offers the best option for land cover mapping. of late, microwave remote sensing is increasingly utilized for land cover discrimination due to its all time, all weather capability. Synthetic Aperture Radar (SAR) Interferometry has significantly increased the potential of microwave remote sensing for land cover mapping. A study was conducted to assess the potential of SAR Interferometry for land cover discrimination using C-band ERS-1/2 SAR data in the Sind river basin, Madhya Pradesh. Use of SAR Interferometric products namely coherence and intensity for land cover classification in the study area gave an overall accuracy of 75%. The coherence alone could discriminate between vegetated and non-vegetated land covers. The vegetation types were found to be negatively affecting the coherence of the area, but, there was no direct negative relationship between coherence and Normalized Difference Vegetation Index (NDVI).

Key words: Synthetic Aperture Radar, Interferometry, Intensity, Coherence, Land cover classification

Introduction

Accurate mapping of land cover type is essential in a number of scientific disciplines and more particularly in environmental monitoring. Conventional ground based surveys of land cover mapping are prohibitively expensive due to involvement of large areas. Production of land cover maps from remotely sensed images has always been perceived as one of the greatest contribution of earth observation by satellites (Mumford *et al.* 1996; Barnsley *et al.* 1995; Higgins 1995). Optical satellite remote sensing methods are more appropriate, but require cloud free conditions for the data to be useful (Srivastava *et al.* 2006; Loveland *et al.* 1991). In tropical areas, cloud free acquisitions are rare, thereby reducing the optical sensors applicability in such areas. Radar, operating in the microwave window of the electromagnetic spectrum offers a solution to the cloud cover problem in that radar data acquisition is independent of cloud cover (Srivastava *et al.* 2006; Raucules *et al.* 2003; Bush *et al.* 1978). Moreover, radar is an active system making the data acquisition possible at any time. Coherence is an estimate of phase stability of the

imaged targets in the time between two SAR data acquisitions. The normalized coherence is given by the complex correlation between two co-registered complex SAR images of backscatter intensities I_1 and I_2 , according to the equation (Weydahl 2001):

$$\gamma = \frac{\langle I_1 I_2^* \rangle}{\sqrt{\langle I_1 I_1^* \rangle \times \langle I_2 I_2^* \rangle}} \quad (1)$$

The brackets $\langle \rangle$ indicate the estimated ensemble average and * denotes the complex conjugate.

Measurement of interferometric coherence and the backscatter intensity can significantly improve the potential of SAR data for land cover classification (Xiaobing *et al.* 2009). Satellite repeat-pass of a few days should be used when carrying out land cover discrimination using Interferometric SAR (InSAR). If the ground surface is undergoing changes caused by glacier motion, thawing conditions, moisture changes, field operations, or building constructions will cause the coherence to decrease (Weydahl 2001). Coherence can also decrease if the signal has a significant volumetric component, as is often the case for

*Corresponding Author Email:shelton_padua@yahoo.com

forested areas and dense shrubs. This variation of coherence could be utilized to classify the vegetated areas and monitor land use changes (Wegmuller and Werner 1997).

Materials and Methods

Study area

The study area is represented by the toposheet 54K/5 of Survey of India (SOI), covering a part of the Sind river basin, Madhya Pradesh. The latitude of the area is $25^{\circ}45'$ to $26^{\circ}0'$ N and the longitude is $78^{\circ}15'$ to $78^{\circ}30'$ E. The area comes under the agro ecological region: Hot semiarid ecosystem (N8D2) (Sehgal *et al.* 1990). Soil is alluvium derived and the length of growing period is 90-150 days. It is primarily an agricultural area and the main crops are wheat and mustard and in some places sugar cane is cultivated. It is a ravine area with rocky outcrops at places. At the time of satellite pass, the main crops were either harvested or at senescence stage.

Data sets

ERS-1 SAR Single look complex (SLC) data was acquired over the area on April 11, 1996 (master image, Fig. 1). The orbit number was 24785 and the frame number was 3087. ERS-2 SAR SLC data was acquired on April 12, 1996 (slave image) with the orbit no 5112 and frame number 3087. ERS-1/2 gives data at C-band, VV polarization and 23° incidence angle. Perpendicular base line for the scenes is 104 m. Spatial resolution of ERS-1/2 intensity image is 30 m. IRS-1B LISS-II multispectral optical data was also acquired for the same area. Spatial resolution of LISS-II data is 36.25 m and the band specifications are as follows; B1: $0.45 - 0.52 \mu\text{m}$, B2: $0.52 - 0.59 \mu\text{m}$, B3: $0.62 - 0.68 \mu\text{m}$ and B4: $0.77 - 0.86 \mu\text{m}$. The date of acquisition was April 7, 1996. Two scenes of LISS-II data (path and row 27/49 and 27/50) were acquired, mosaic was made and the area corresponding to the study region was extracted.

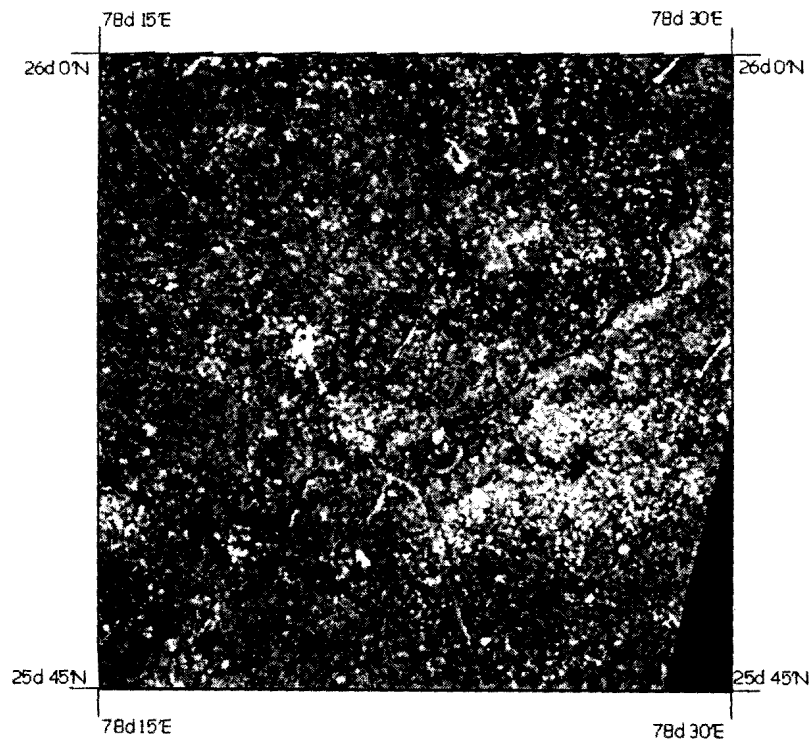


Fig 1. Intensity image (11, April 1996) of the Sind region derived from ERS-1 SAR SLC data (master image)

Land cover classification

The intensity and coherence images were generated using the Earth View APP and EV InSAR software. SLC image was transformed to intensity image through a composite processing. SLC images are in slant range coordinates and

each pixel is represented by complex numbers to preserve the magnitude and phase information. The multi-look processing was applied on the SLC image. The multi-looked image was generated by averaging the power (square of absolute value of the complex image) across a number of

lines in both the azimuth and range directions. The multi-look intensity image was created with 5 Azimuth looks and 1 Range look which is generally used for ERS satellites. The number of looks are chosen in order to obtain a sampling of the multi-look image which gives almost square pixels (the ground range length and azimuth length are almost equal). Then speckle processing was carried out to reduce the radar noise after which geocoding was done to transform the image from radar coordinates into WGS84 coordinates (Parcharidis *et al.* 2007; Laur 2004; Sarmap 2008). The coherence value, which is the correlation between the master and slave phase information was derived as per the equation 1 after coregistering the master and slave images. The coherence value ranges from 0 to 1. A high coherence value means a high correlation of the image elements (Weydahl 2001). These interferometric products were used for land cover classification. The coherence map (Fig. 2) and the intensity information of the master and slave images were taken as three bands and supervised classification was done to get the

land cover. For the intensity images, speckle suppression was done using Gamma 5x5 filter before the signature extraction and image classification (Taubenböck *et al.* 2012; Ban 2003; Congalton 1991). The land cover categories were determined based on the ground truth survey of the area. Other ancillary information was collected from Survey of India map (54K/5) in conjunction with standard FCC prepared from IRS-1B LISS-II data. The land cover types identified were degraded forest, eucalyptus plantations, sugarcane fields, water body, open land, harvested fields, and eroded land. Bitmaps were created for each training site, which were used in extracting the statistics for each of the land cover classes. Signature separability analysis for the land cover classes was done using Bhattacharya Distance method. The supervised classification algorithm used was Maximum likelihood classifier. The classification accuracy was assessed using error matrix and Kappa coefficient (K). The K values can range from +1 to -1. Positive values of K occur from greater than chance agreement while negative values indicate a less than chance agreement (Skidmore and Turner 1989).

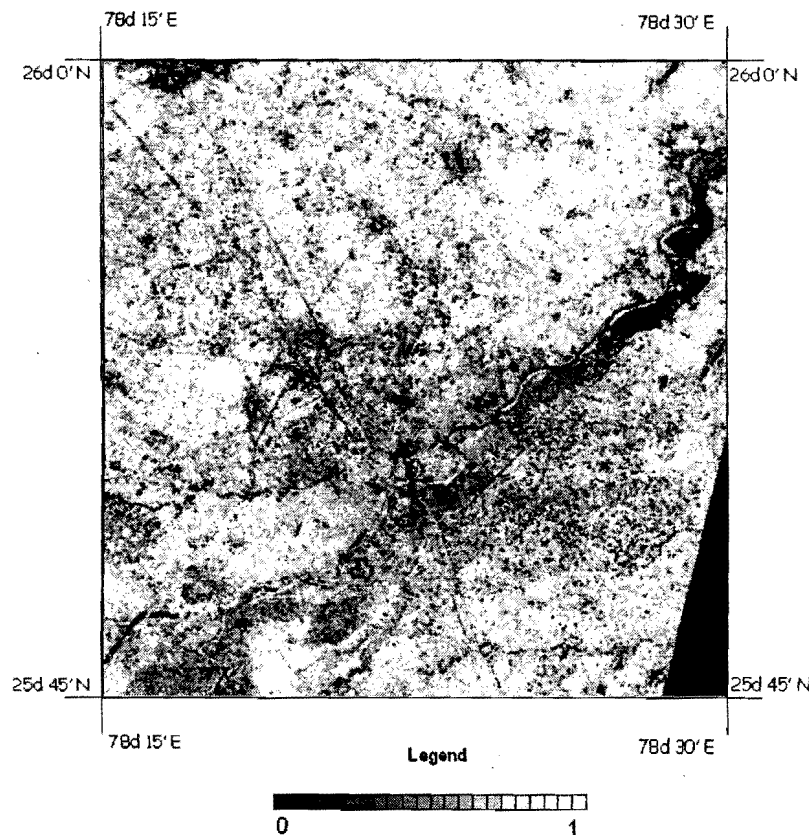


Fig 2. Coherence map (12, April 1996) of Sind region derived from ERS-1/2 tandem data

Results and Discussions

Land cover signatures

The variation of coherence with respect to the land cover types is shown in Fig. 3 and the error bars indicate the standard deviation. The lowest value of coherence was for water (0.185 ± 0.103) and the highest value was for open land (0.873 ± 0.027). All the land cover types with little or no vegetation had higher values of coherence and land covers with vegetation gave lower values of coherence. In nature, both surface and volume scattering contributes to the radar backscatter and the presence of volume scattering decreases the coherence (Hagberg *et al.* 1995). There is comparatively high variation of coherence in land cover types namely degraded forest, eucalyptus plantation and sugarcane fields. This may be due to changes in the response of different plant canopies to the stress caused by the drag force of wind. The role of rain in causing decorrelation was ruled out, as there

was no rain within the one-day gap of acquisition of ERS-1/2 tandem data. Wind can move vegetation parts like leaves and branches by a distance up to a wavelength (for C-band) or more, which would result in a phase change of one cycle or more enough to cause decorrelation (Seynat and Hobbs 1998).

One of the reasons for loss of coherence in vegetated areas is due to the growth of vegetation. But in this study, since the coherence map was generated using the tandem data (Fig. 1 and 2), contribution of vegetation growth to the loss of coherence could be ruled out. The reason could be wind (meteorological factors) changing the leaf and branch positions. Reason for change in the level of coherence between different vegetation types *i.e.* eucalyptus, sugarcane and degraded forest could be the difference in response of the vegetation types to the drag force of wind because of differences in plant structure and its mechanical strength (Hobbs *et al.* 1998).

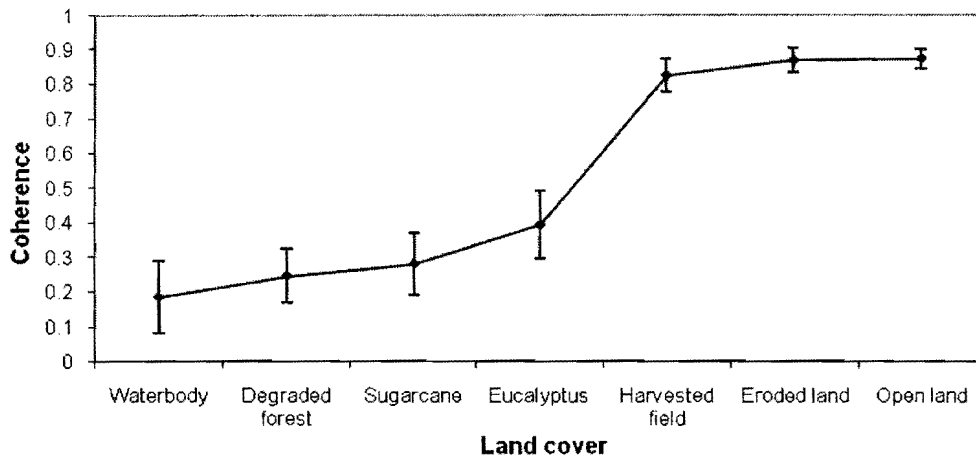


Fig 3. Variation of coherence with different land cover types.

Note:-Error bars indicate \pm standard deviation

It is noticeable that eucalyptus plantation is having higher coherence among vegetated areas (Fig. 3) followed by sugarcane and degraded forest. In the area denoted as degraded forest, there was only one main plant species namely *Acacia sp.* (babul plant), which is shrubby in nature with small leaves. Out of the three vegetated land cover types, eucalyptus was the sturdiest one and its response to wind would be minimal compared to other two land cover types. Due to the very reason, the effect of wind causing decorrelation in eucalyptus areas could have been less and

hence eucalyptus covered areas gave a higher coherence compared to sugarcane and degraded forest. But in case of sugarcane and babul plant, being a shrub, babul has more strength than sugarcane, which is a grassy plant with very long leaf blades. As per the above explanation, sugarcane (coherence was 0.28) should have given a low coherence compared to degraded forest (0.25). But that was not the case. Under field conditions, when sugarcane crop attains fully developed canopy, leaf blades and tillers are so closely placed and touch each other that there is hardly any space for

independent movement leading to loss of coherence. This high density of sugarcane plants might have changed the response pattern to wind and stronger wind would be required to cause change of positions of the plant parts. In case of degraded forest, canopy was comparatively open resulting in higher volumetric scattering and moreover the leaves were smaller and there was enough room for the movement of branches and leaves in response to wind. This may be the possible explanation for slightly lower coherence for land cover type like degraded forest compared to sugarcane.

Water body gave lowest coherence (0.185 ± 0.103) values due to the fact that changing wind condition (meteorological conditions) over water can lead to very different backscattering behaviours (Strozzi *et al.* 2000) and also due to low signal to noise ratio (Wegmuller and Werner 1995). In case of non-vegetated land covers, there was not much separation between the mean values of coherence for different classes namely open land, eroded land and harvested fields. This may be due to the fact that in these three classes, the soil surface was being sensed and the coherence

information was that of soil surface. Gaveau (2002) opined that in optimal practical circumstances the observed coherence hardly ever exceeds 0.95 over smooth and stable bare surface. The coherence value for open land was 0.873 ± 0.027 and that for eroded land was 0.869 ± 0.034 . These almost identical values may be due to the fact that there was no decorrelation effect due to vegetation and also due to the tandem acquisition of the data. In case of the harvested fields, the coherence is still less (0.824 ± 0.047). In our study area, there were stubbles and senesced crops in the field, which might have contributed a little to the volume scattering and hence a small decrease in the coherence compared to open land.

From (Fig 3), it is very clear that the vegetated and non-vegetated areas could be separated out using the coherence information alone. Water body was also moderately separable from the vegetation classes (Table 1). But if we include more land cover categories, it may become difficult to get a good land cover separation as the signature means within the vegetated and non-vegetated land cover types may overlap making separation ambiguous.

Table 1. Separability index (Bhattacharya Distance) for land cover classes when information from coherence and master intensity images were considered

	Eroded land	Eucalyptus	Harvested field	Open land	Water body	Sugar cane
Forest	2.00	1.27	2.00	2.00	1.91	0.14
Sugarcane	2.00	0.86	2.00	2.00	1.77	-
Water body	2.00	1.90	2.00	2.00	-	-
Open land	0.09	2.00	0.52	-	-	-
Harvested field	0.44	1.98	-	-	-	-
Eucalyptus	2.00	-	-	-	-	-

Variations of coherence and intensity values from master and slave images for different land cover types are presented in (Fig 4). As expected water body gave the lowest intensity values for both the master and slave images. From (Fig 4), it can be seen that both master and slave intensity values followed the same trend. But, one noticeable feature in the figure is that the degraded forest gave higher values than that of open land. The degraded forest canopy was not closed and

it might have allowed the radar waves to enter into it and the tree trunks might have acted as a source for double bounce returning the radar signal back to the antenna resulting in higher intensity. Open land, which was dry, resulted in low backscatter. In case of eroded land the rugged nature of the ravine lands might have caused an overall less backscatter due to shading effects. In case of sugarcane and eucalyptus, varying levels of volume scattering is responsible for low intensity values.

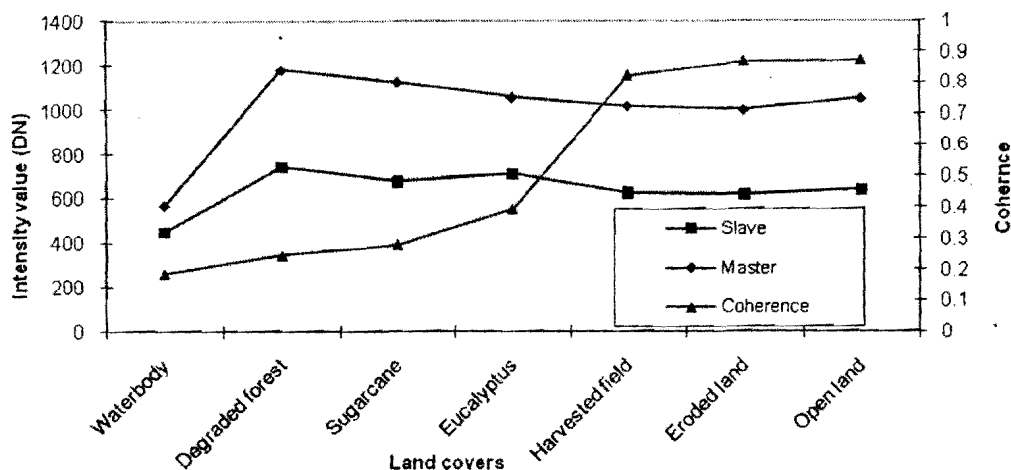


Fig 4. Comparison of land cover signatures between master and slave intensity images and coherence image.

To improve the land cover separability, intensity information from the master and slave images were also included along with coherence information in the analysis. The Bhattacharya Distances for different land cover classes are presented in (Table 1 and 2). Maximum separability of 2 was between non-vegetated land cover types (open land, eroded land and harvested field) & vegetated land cover types (eucalyptus, sugarcane and degraded forest) and non-vegetated land cover types & water body. But the separation within the non-vegetated land cover types and that within the vegetated land cover types were very poor. The lowest

separability was between eroded land and open land (0.09). Improper combinations of image bands and/or training sites, which have large internal variability, can cause low signature separability (Richards 1986). In this case, the two land cover types were having almost same kind of signatures making it difficult to separate. So in nutshell, the land cover types, open land and eroded land statistically fall under the same category. Other land cover types, which gave poor separability, were harvested field & eroded land (0.44), open land & harvested fields (0.52), degraded forest & sugarcane (0.14) and sugarcane & eucalyptus (0.86).

Table 2. Separability index for land cover classes when coherence, master and slave intensity images were used

	Eroded land	Eucalyptus	Harvested field	Open land	Water body	Sugar cane
Forest	2.00	1.34	2.00	2.00	1.98	0.30
Sugar cane	2.00	1.06	2.00	2.00	1.83	-
Water body	2.00	1.97	2.00	2.00	-	-
Open land	0.17	2.00	0.55	-	-	-
Harvested field	0.55	1.99	-	-	-	-
Eucalyptus	2.00	-	-	-	-	-

It was also found that (Table 2) addition of slave intensity image did not improve the separability of poorly separated classes, except for sugarcane and eucalyptus, where the separability index got improved to 1.06 (to get a moderate

separability between the classes, the separability index should be at least greater than one). For other poorly separated classes, there was some slight improvement but it was not enough to make the index above one. The reason

could be both the intensity bands were giving the same kind of information. Since the data used was ERS-1/2 tandem pair, we cannot expect much change in the intensity values of different land cover types. Had there been rain between the one-day period in the acquisition of master and slave images, we could have expected some change in the intensity recorded by the master and slave. But, that was not the case. However for water body this can happen, since wind can lead to very different backscattering behaviour for water bodies. A calm water body appears dark in a radar image because the water surface acts as a perfect reflector, sending the radar signal away from the sensor. When the surface of the water is ruffled, reflective facets that are formed, comparable in size to the radar wavelength, become non directional and transmit part of the energy back to the radar. Some of these facets may

even face the radar, especially for small angle of incidence such as that used by ERS-1 and in such cases water appear bright (Bruzzone 2004; Massonnet and Feigl 1998). In the present study, lowest intensity was observed for water body for both the master and slave images. However, coherence image and master intensity image were enough to give ample discrimination of water body from other land cover types.

Relationship between Coherence and Vegetation

The Normalized Difference Vegetation Index image was generated from the IRS LISS-II data and it was accurately co-registered with the coherence map. The variation of coherence map with reference to the NDVI image was analyzed (Tables 3 and 4). The range of coherence in the image was 0 to 0.949 and that of NDVI was -0.475 to 0.42.

Table 3. Variation of coherence and NDVI with respect to different land cover types

Class name	Min.		Max.		Mean		SD	
	Coh.	NDVI	Coh.	NDVI	Coh.	NDVI	Coh.	NDVI
Water body	0.031	-0.423	0.446	-0.010	0.185	-0.283	0.103	0.088
Forest	0.036	0.138	0.452	0.225	0.246	0.177	0.077	0.016
Sugar cane	0.060	0.261	0.444	0.417	0.280	0.314	0.090	0.035
Eucalyptus	0.226	0.084	0.546	0.151	0.395	0.121	0.098	0.020
Harvested field	0.654	-0.022	0.921	0.094	0.824	0.035	0.047	0.026
Eroded land	0.764	0.000	0.946	0.160	0.869	0.082	0.035	0.028
Open land	0.785	-0.057	0.943	0.066	0.873	-0.009	0.028	0.024

Table 4. Relation between Coherence and NDVI under different land cover classes

Class name	Correlation coefficient	Regression equation
Water body	0.49	$Y = 0.72x + 0.47$
Forest	-0.45	$Y = -1.81x + 0.65$
Sugar cane	-0.4	$Y = -0.44x + 0.85$
Eucalyptus	-0.60	$Y = -1.85x + 0.77$
Harvested field	-0.13	$Y = -0.20x + 0.82$
Eroded land	0.40	$Y = 0.63x + 0.77$
Open land	0.31	$Y = 0.74x + 0.85$
Total image	-0.22	$Y = -0.49x + 0.80$

Correlation between NDVI and coherence for eucalyptus was -0.6 . Eucalyptus plants gave a comparatively high NDVI value (0.121) and at the same time coherence value for eucalyptus was relatively low (0.395), resulting in negative correlation for this class. Forest gave a negative correlation of (-0.45) and that for sugarcane was (-0.4). The last two classes also showed negative correlation due to the same reasons as for the eucalyptus plants. Even though, NDVI values were higher for sugarcane (0.314) and degraded forest (0.177) in comparison to eucalyptus, the negative correlation of coherence with NDVI for these classes was less than that of eucalyptus. Sugarcane gave highest value for NDVI and lesser value for coherence (0.280), but the correlation was found less negative than that of eucalyptus, which got a negative correlation of (-0.60). Under such situation one would expect the correlation to be more negative than that for eucalyptus. But that was not the case. This could be due to the fact that the corresponding pixel in the coherence image and NDVI image are not following a definite relation. Higher NDVI value in one pixel did not necessarily mean a lower coherence value in the corresponding pixel. In nutshell, the relation between coherence and NDVI is not a simple one.

Harvested fields gave a correlation of (-0.13). Coherence was high in this case (0.824) and the NDVI was low (0.035) compared to the above three classes. Water gave a correlation of (0.49). In case of water, coherence was lowest (0.185) and NDVI was negative (-0.283). Since both were low, a positive correlation was obtained. Open land and eroded land gave correlation of (0.31) and (0.4), respectively. Coherence was high for both the classes and

NDVI close to zero. But for the total image, correlation was found to be (-0.22). A careful analysis of above results would reveal that NDVI is not the only factor / major factor in determining the coherence response of the class. NDVI speaks about the vegetation vigour and which has some effect on the coherence, but NDVI does not throw any light into the mechanical behaviour of leaves and branches, which are more important in determining the coherence of the area in response to meteorological factors like wind. The maximum correlation obtained was (-0.6) and R^2 (coefficient of determination) would come to 0.36. So, to the maximum extent, only 36 percent of the variability of coherence is explained by NDVI. NDVI is influenced by green biomass and it can in turn influence volume scattering, which is one of the factors affecting coherence.

Land cover classification

The coherence and master intensity images (Fig. 1 and 2) were used as two channels for the supervised classification. To improve the classification accuracy, the classes, eroded land and open land, which gave very low separability index of 0.09, were merged to one class. Low separability index is obtained when two classes are not statistically separable and the best way to improve the classification accuracy is to merge the classes, which give least separability. The classification results are presented in (Table 5 and 6). The class sugarcane gave the lowest accuracy (36.26) and water body gave the highest accuracy (99.3). We can see that the overall accuracy for the classification is 74.4% and the Kappa coefficient is 0.67, which represents a good agreement. The overall accuracy is not bad, when there is no other means for obtaining the land cover information.

Table 5. Confusion matrix for land cover classification when coherence and master intensity images were used for classification

Class name	Pixels	Percent Pixels classified					
		Eucalyptus	Forest	Water body	Open land	Sugarcane	Harvested field
Eucalyptus	25	90.91	0.00	0.00	0.00	9.09	0.00
Forest	2845	10.35	69.6	0.00	0.00	20.04	0.00
Water body	566	0.00	0.00	99.3	0.00	0.70	0.00
Open land	2000	0.00	0.00	0.00	86.19	0.00	13.81
Sugarcane	144	16.48	45.05	2.20	0.00	36.26	0.00
Harvested field	343	0.72	0.00	0.00	34.45	0.00	64.83

Overall accuracy = 74.4%; KAPPA = 0.67

For improvement in the overall accuracy, both master and slave imagery information was coupled with coherence information and the classification results are given in Table 6 and Fig. 5. The overall accuracy was 75.25% and the Kappa

coefficient was 0.68. The additional slave image information did not improve the overall classification significantly. This is because the slave and master images provide the same kind of information to the classification process.

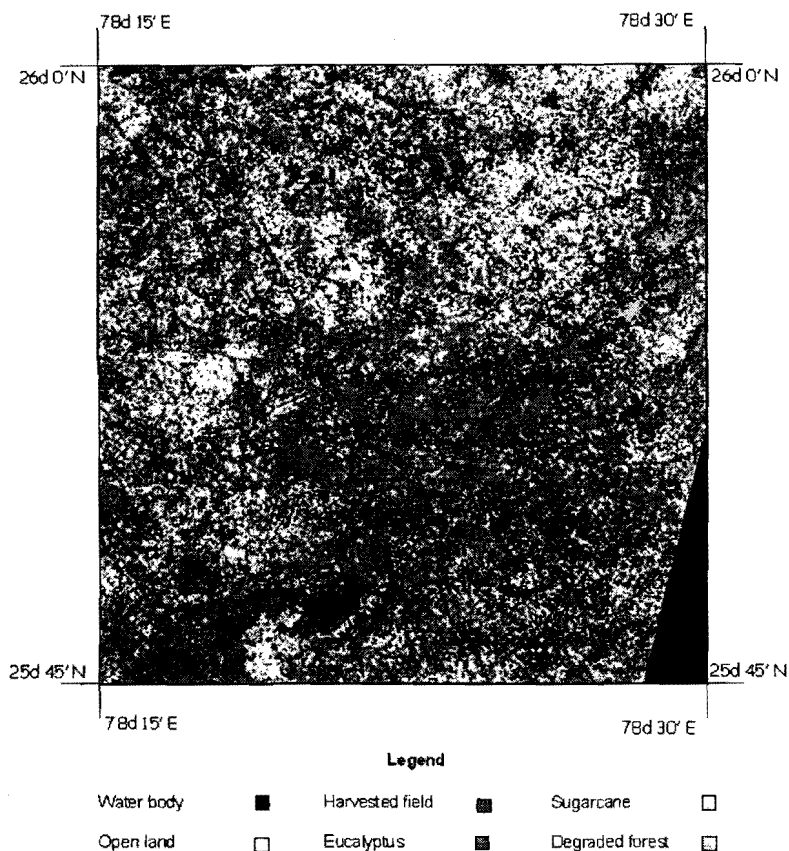


Fig 5. Land cover map (12, April 1996) of Sind region derived from SAR Interferometric products.

Table 6. Confusion matrix for land cover classification when coherence, master and slave images were used for classification

Class name	Pixels	<i>Percent Pixels classified</i>					
		Eucalyptus	Forest	Water body	Open land	Sugar cane	Harvested field
Eucalyptus	25	86.36	0.00	0.00	0.00	13.64	0.00
Forest	2845	10.35	74.67	0.00	0.00	14.98	0.00
Water body	566	0.00	0.00	98.60	0.00	1.4	0.00
Open land	2000	0.00	0.00	0.00	86.80	0.00	13.20
Sugar cane	144	15.38	52.75	2.20	0.00	29.67	0.00
Harvested field	343	0.72	0.00	0.00	35.41	0.00	63.88

Overall accuracy = 75.26%; Kappa = 0.68

Conclusions

Using SAR interferometric products, an overall accuracy of 75% was obtained for land cover type discrimination. The Coherence information alone could discriminate well between vegetated and non-vegetated land cover types. But there is overlap of coherence values within vegetated and non-vegetated land cover types. When coherence information and intensity information from master image were considered, a moderate separability between the different land cover types could be obtained. With the addition of intensity information from the tandem slave image, classification accuracy could not be improved significantly. Hence, SAR data may not be cost effective, unless SAR data is preferred to avoid interference of clouds. In general, the relation between NDVI and the Coherence of SAR images is negative. NDVI does not appear to be a good index to characterize vegetation in terms of decorrelating the SAR images.

Acknowledgements

Authors are thankful to Sierra Atlantic Ltd., Hyderabad, for helping in carrying out Interferometric studies using their facility. We acknowledge Mr. Girish Kumar and Mr. T.S. Rao of Sierra Atlantic for sparing time to help in the SAR data analysis.

References

- Ban, Y. (2003). Synergy of multi temporal ERS-1 SAR and Landsat TM data for classification of agricultural crops. *Canadian Journal of Remote Sensing* **9(4)**, 518-526.
- Barnsley, M. J., Barr, S. L. and Tsang, T. (1995). Producing large-area land cover maps from satellite sensor images: scaling issues and generalisation techniques., In *Environmental Remote Sensing from regional to global scales*, edited by G. Foody, and P. Curran, John Wiley & Sons.
- Bruzzone, L. (2004). An Advanced System for the Automatic Classification of Multitemporal SAR Images. *IEEE Transactions on Geoscience and Remote Sensing* **42(6)**, 1321-1334.
- Bush, T.F. and Ulaby, F.T. (1978). An evaluation of radar as a crop classifier. *Remote Sensing of Environment* **7(1)**, 15-36.
- Congalton, R. (1991). A review of assessing the accuracy of classifications of remotely sensed data. *Remote Sensing of Environment* **37**, 35-46.
- Gaveau, D.L.A. (2002). Modelling the dynamics of ERS-1/2 coherence with increasing woody biomass over boreal forests. *International Journal of Remote Sensing* **23(18)**, 3879-3885.
- Hagberg, J.O., Ulander L.M.H. and Askne J. (1995). Repeat-pass SAR Interferometry over forested terrain. *IEEE Transactions on Geoscience and Remote Sensing* **33(2)**, 31-340.
- Higgins, N.A. (1995). Potential of the ATSR-2 on ERS-2 for monitoring land cover change. In 21st Annual Conference of the UK Remote Sensing Society, edited by P.J. Curran, and Y.C. Roberston, pp. 320-324, Remote Sensing Society, University of Southampton, 11-14 September.
- Hobbs, S.E., Ang, W., and Seynat, C. (1998). Wind and rain effects on SAR backscatter from crops. Proc. 2nd International workshop on Retrieval of bio and geophysical parameters from SAR data for land applications, ESTEC, The Netherlands, 21-23 October, 1998.
http://earth.esa.int/services/esa_doc/_sp441/PAGE_S/papers/P053.PDF
- Laur, H., Bally, P., Meadows, P., Sanchez, J., Schaettler, B., Lopinto, E. and Steban, D. (2004). ERS SAR Calibration: Derivation of the Backscattering Coefficient σ^0 in ESA ERS SAR PRI Products. Document No: ES-TN-RS-PM-HL09, Issue 2, Rev. 5f
- Loveland, T.R., Merchant, J.W., Ohlen, D.O. and Brown, J.F. (1991). Development of a Land Cover Characteristics Database for the Conterminous US, *Photogrammetric Engineering and Remote Sensing* **57(11)**, 1453-1463.
- Massonnet, D. and Feigl, K.L. (1998). Radar interferometry and its application to monitor changes in the earth's surface. *Reviews of Geophysics* **36(4)**, 441—500.
- Mumford, B., Muller, J.P. and Mandanayake, A. (1996). Assessment of land cover mapping potential in Africa using tandem ERS Interferometry. In Proceedings of the "Fringe96" workshop on ERS SAR Interferometry, Zurich, 30 Sept - 2 Oct 1996, pp179-188, ESA SP-406, March 1997 (ISBN92-9092-307-5).

- Parcharidis I., Delladetsimas P. and Kourkouli P. (2007). ERS SAR power satellite image interpretation and urban characteristics: the case of Athens, Proceedings of 8th Pan-Hellenic Geographical Conference of the Hellenic Geographical Society, Athens, October 4-7, 2007. p. 71-76.
https://pkourkouli.files.wordpress.com/2010/12/ge_o_conference_07.pdf
- Raucules, D., Le Mouélic, S., Carnec, C., King, C. (2003). Urban subsidence in the city of Prato (Italy) monitored by satellite radar interferometry. *International Journal of Remote Sensing* **20**, 891-897.
- Richards, J.A. (1986). *Remote Sensing Digital Image Analysis*. Springer-Verlag, Berlin, Heidelberg, New York, London, Paris, Tokyo, 206-225.
- Sarmap, (2008). SARscape: The Earth Observation Information Gateway. Technical Description in a Nutshell.
http://www.exelisvis.com/portals/0/pdfs/envi/sarscape_technicaldescription.pdf
- Sehgal, J., Mandal, D. K, Mandal, C. and Vadivelu, S. (1990). India: Agro-Ecological Regions. National Bureau of Soil Survey and Land Use Planning, Nagpur.
- Seynat, C. and Hobbs, S.E. (1998). Crop parameter retrieval from multi-temporal SAR coherence images. Proc. 2nd International workshop on Retrieval of bio and geophysical parameters from SAR data for land applications, ESTEC, The Netherlands, 21-23 October, 1998.
<http://www.estec.esa.nl/conferences/98c07/papers/P052.PDF>
- Skidmore, A. and Turner, B. (1989). Assessing the accuracy of resource inventory maps. In : Proceedings of Global Natural Resource Monitoring and Assessment : Preparing for the 21st Century, Venice, Italy, 524-535.
- Srivastava, H. S., Patel P. and Ranganath, R. N. (2006). Application potentials of synthetic aperture radar interferometry for land-cover mapping and crop-height estimation. *Current Science* **91(6)**, 783-788.
- Strozzi, T., Dammert, P.B.G., Wegmuller, U., Martinez, J.M., Askne, J.I.H., Beaudoin, A. and Hallikainen, M.T. (2000). Land use mapping with ERS SAR interferometry. *IEEE Transactions on Geoscience and Remote Sensing* **38(2)**, 766-775.
- Taubenböck, H., Felbier, A., Esch, T., Roth, A., Dech, S. (2012). Pixel-based classification algorithm for mapping urban footprints from radar data: a case study for RADARSAT-2. *Canadian Journal of Remote Sensing*, Published on the web 02 April 2012
- Wegmuller, U. and Werner, C.L. (1995). SAR Interferometric signatures of forest. *IEEE Transactions on Geoscience and Remote Sensing* **33(5)**, 1153-1161.
- Wegmuller, U. and Werner, C.L. (1997). Retrieval of vegetation parameters with SAR Interferometry. *IEEE Transactions on Geoscience and Remote Sensing* **35(1)**, 18-24.
- Weydahl, D.J., (2001). Analysis of ERS SAR coherence images acquired over vegetated areas and urban features. *International Journal of Remote Sensing* **22(14)**, 2811-2830.
- Xiaobing Zhou, Ni-Bin Chang and Shusun Li. (2009). Applications of SAR Interferometry in Earth and Environmental Science Research *Sensors* **9**, 1876-1912, doi: 10.3390/s90301876.